

特约专栏

## Mechanism of Reorientation and Redistribution of Multi-Variants in Shape Memory Alloys under External Field

CUI Yanguang, WAN Jianfeng, MAN Jiao, ZHANG Jihua, RONG Yonghua  
(School of Materials Science and Engineering, Shanghai Jiao Tong University, Shanghai 200240, China)

**Abstract:** The mechanism of reorientation and redistribution of martensitic multi-variants under the cyclic stress was studied by using Phase-Field method. The results showed that under the small loading, the twin boundary migration is the main mechanism and three variants can be kept in the system, with the increase of external stress, the nucleation and growth of parent at the twin interface is the main mechanism to realize the reorientation of 3→2 variants. After removing the loading, the vanished variant nucleates at the twin boundary to perform the redistribution of inner microstructure in the system. This kind of mechanism controls the shape memory effect of the Mn-Cu alloy during the cyclic loading.

**Key words:** reorientation; multi-variants; stress; twin boundary; phase-field

**CIC number:** TG139+.6 **Document code:** A **Article ID:** 1674-3962(2012)03-0039-04

## 形状记忆合金中的马氏体变体在外场下的再取向和再分布机制

崔严光, 万见峰, 满蛟, 张骥华, 戎咏华

(上海交通大学材料科学与工程学院, 上海 200240)

**摘要:** 利用相场方法研究了马氏体变体在循环应力作用下再取向和再分布的微观机制。模拟结果表明, 随着外应力的增加, 在孪晶界面会出现母相的形核和长大, 以此实现变体间的转化, 这是3种变体转化为2种变体的主要再取向机制; 卸载后消失的变体在孪晶界面重新形核并长大以完成系统内微观组织的再分布。在Mn-Cu合金中这种机制是控制循环载荷下形状记忆效应产生的主要机制。

**关键词:** 再取向; 多变体; 应力; 孪晶边界; 相场

### 1 Introduction

The martensitic twin boundary (TB) migration in Mn-based alloys is associated with the shape memory effect (SME)<sup>[1-2]</sup> and the high damping effect<sup>[3]</sup>. The martensitic variants can reorientate and redistribute under the stress and magnetic field, which makes a great contribution to the field-induced large strain output in the micromechanical devices. Experimental observations showed that one variant transformed into another variant through TB motion if the external field was applied to the materials<sup>[3-4]</sup>. This kind of interfacial migration and reorientation was also found in other systems with ferroelectric, ferroelastic, magnetic domains<sup>[5]</sup>. However, if the system includes only one martensite variant, no strain can be outputted under the external field due to the

lack of TB migration. It is still unknown how the reorientation of multi-variants ( $> 2$ ) under the external field affects the strain output in the system. Phase-field method is powerful and successful to simulate the micro-structural evolution of phase transition<sup>[6]</sup>. External field was employed into the Phase-field simulation so as to study the stress-induced structural transformation in martensitic alloys<sup>[7-8]</sup>. Their work emphasizes on the phase transition under the constrain and paid little attention to the mechanism of reorientation and redistribution of variants under the stress after the occurrence of martensitic transformation.

In this paper, a twin boundary model was introduced into the 3-D phase-field method to study the migration of twin-boundary. The main purpose is to investigate the mechanism of reorientation and redistribution of martensitic variants under the cyclic stress. The results of simulation show that under the small loading, the twin boundary migration is the main mechanism and three variants can be kept in the system. When the big stress is applied to the system, three variants can turn to two variants. The parent will nucleate at the twin-boundary and grow quickly, then transform into two variants through martensite/parent interface. After removing

Received date: 2012-01-16

Foundation item: National Key Basic Research Program(2012CB619400);  
National Natural Science Foundation(51171112)

Biograph: Cui Yanguang, Borned in 1987, Doctor

Corresponding author: Rong Yonghua, Borned in 1950, Professor

loading, the vanished variant will nucleate and grow at the twin boundary. The cyclic loading and energy variation were also considered to explain this mechanism, which will be helpful for the design of high-damping and super-elastic alloys in the engineering applications.

## 2 Methods

The total Ginzburg-Landau (GL) free energy of the system ( $F$ ) is the sum of chemical free energy ( $F_{ch}$ ), interfacial energy ( $F_{TB}$ ) and elastic strain energy ( $F_{el}$ ), and will be in the form<sup>[9]</sup> of

$$F = F_{ch} + F_{TB} + F_{el} \quad (1)$$

$$F_{ch} = \frac{1}{2}A(\eta_1^2 + \eta_2^2 + \eta_3^2) - \frac{1}{3}B(\eta_1^3 + \eta_2^3 + \eta_3^3) + \frac{1}{4}C(\eta_1^2 + \eta_2^2 + \eta_3^2)^2 \quad (1-a)$$

$$F_{el} = \frac{1}{2} \sum \int \frac{d^3k}{(2\pi)^3} B_{pq}(\vec{e}) \{ \eta_p(r) \}_k^* \{ \eta_q(r) \}_k + \kappa \sum_p \sigma_{ij} \varepsilon_{ij}^0(p) \eta_p(r) \quad (1-b)$$

$$B_{pq}(\vec{e}) = C_{ijkl}(p) \varepsilon_{kl}^0(q) - e_i \sigma_{ij}^0(p) \Omega_{kl}^0(\vec{e}) \sigma_{kl}^0(q) e_l \quad (1-c)$$

in which  $A$ ,  $B$  and  $C$  are the Landau-free-energy coefficients, which meet the global minimum condition at  $\{ \eta_1, \eta_2, \eta_3 \} = (\eta_0 \ 0 \ 0) = (0 \ \eta_0 \ 0) = (0 \ 0 \ \eta_0)$  corresponding to three tetragonal martensitic variants.  $\{ \eta_p(r) \}_k^*$  is the complex conjugate of  $\{ \eta_p(r) \}_k$  (the Fourier transformation of  $\eta_p(r)$ ).  $B_{pq}(\vec{e})$  is a two-body interaction potential.  $\sigma_{ij}^0(p) = C_{ijkl} \varepsilon_{kl}^{00}(p)$ , in which  $C_{ijkl}$  is the elastic constant and  $\varepsilon_{kl}^{00}(p)$  is the corresponding stress-free strain for the  $p$ th variant.  $\vec{e} = \vec{k}/k$  ( $\vec{k}$  is a reciprocal lattice vector).  $\Omega_{ij}(\vec{e})$  is a Green function tensor being inverse to the tensor  $\Omega_{ij}^{-1}(\vec{e}) = C_{ijkl} e_k e_l$ , in which  $e_k$  is the  $k$ th component of  $\vec{e}$ . The external stress  $\sigma_{ij}$  is simplified to be  $\sigma_0$  (et. along  $z$ -direction).  $\kappa = 1$  means applying tensile stress and  $\kappa = 0$  means removing external stress. At the present model<sup>[6]</sup>, the twin boundary could not be considered and is always taken as the same expression of martensite/austenite interface. In order to know the twin boundary gradient energy, we can define the order parameter of TB ( $\eta_{TB}$ ) as

$$\eta_{TB} = \lambda \eta_p + (1 - \lambda) \eta_q, \quad (2)$$

Here  $\eta_p$  or  $\eta_q$  is the LOP of  $p$ th or  $q$ th variant.  $\lambda$  varies from 1 to 0, which satisfies the boundary condition; when  $\lambda = 1$ ,  $\eta_{TB} = \eta_p$ ; when  $\lambda = 0$ ,  $\eta_{TB} = \eta_q$  (shown in Figure 1). Then we can write the twin-martensitic boundary energy ( $F_{TB}$ ) in the form,

$$F_{TB} = \int_V (\nabla \eta_{TB})^2 dV = \sum_{p \neq q} \int_V [\nabla (\lambda \eta_p + (1 - \lambda) \eta_q)]^2 dV \quad (3)$$

In the phase-field model, the TDGL (time-dependence-Ginzburg-Landau) equation for the non-conserved structural order parameter  $\eta_p(r, t)$  field variables satisfy the equation:  $\partial \eta_p(r, t) / \partial t = -L \delta F / \delta \eta_p(r, t) + \xi_p(r, t)$ , where  $L$  is the kinetic coefficient for the microstructural evolution,  $\xi_p(r, t)$  denotes the Gaussian-distributed Langevin noise term describing the thermal fluctuation. Combined with Eq. (3), the modified phase-field equation describing the evolution kinetics can be written as

$$\frac{\partial \eta_p(r, t)}{\partial t} = - \{ -L(\nabla^2 [\lambda^2 \eta_p(r, t)] + \sum_{p \neq q} \nabla^2 [\lambda(1 - \lambda) \eta_q(r, t)] + f_{\eta_p}(r, t) \} + \xi_p(r, t) \quad (4)$$

in which  $f_{\eta_p}(r, t) = \partial(F_{ch} + F_{el}) / \partial \eta_p(r, t)$ . It is always convenient to present the above kinetic equation in a reduced form for the numerical simulations. The reduced time and spatial coordinates are defined as  $\tau = L |\Delta f(T)| t$  and  $r_i = x_i / l$ .  $\Delta f(T)$  as the transformation driving force is described by the Clausius-Clapeyron equation as  $|\Delta f(T)| = Q(T_0 - T) / T_0$ , where  $Q$ ,  $T$  and  $T_0$  are the MT (Martensitic Transformation) latent heat, MT temperature, and equilibrium temperature between the parent phase and martensite, respectively.  $l$  is the length unit assigned to the computational grid ( $N_0 \times N_0 \times N_0$ ). Other dimensionless parameters will be chosen to govern the kinetic equation:  $A^* = A / |\Delta f(T)|$ ,  $B^* = B / |\Delta f(T)|$ ,  $C^* = C / |\Delta f(T)|$ ,  $\sigma_{ij}^* = \sigma_{ij} / |\Delta f(T)|$ ,  $L^* = 2L / (l^2 \cdot |\Delta f(T)|)$ ,  $B_{pq}^* = B_{pq} / |\Delta f(T)|$ . By using the semi-implicit Fourier-spectral method proposed by Chen *et al.*<sup>[10]</sup>, the Eq. (3) as a partial differential equation can be transformed into a sequence of ordinary differential equations in the Fourier space in a dimensionless form,

$$\frac{\partial \eta_p(k, \tau)}{\partial \tau} = -L^* k^2 [\lambda^2 \eta_p(k, \tau) + \sum_{p \neq q} \lambda(1 - \lambda) \eta_q(k, \tau)] + f_{\eta_p}^*(k, \tau) - \xi_p^*(k, \tau) \quad (5)$$

Based on the explicit Euler scheme, we proposed the following modified semi-implicit scheme:

$$(1 + \Delta \tau L^* k^2 \lambda^2) \eta_p^{n+1}(k) = \eta_p^n(k) - \sum_{p \neq q} [\Delta \tau L^* k^2 \lambda(1 - \lambda) \cdot \eta_q^n(k)] + \Delta \tau [f_{\eta_p}^*(k) - \xi_p^n(k)] \quad (6)$$

In the simulation we use the Mn-Cu alloys as the example to investigate the twin martensitic system under the cyclic stress, which undergoes the fcc  $\rightarrow$  fct MT<sup>[3]</sup>. The Green tensor ( $\Omega_{ij}(e)$ ) in the elastically isotropic medium equals to  $\delta_{ij}/G - e_i e_j / [2G(1 - \nu)]$ .  $G$  as the shear modulus of Mn-Cu alloys<sup>[11]</sup> is  $31 \times 10^9$  Pa,  $\nu$  as its Poisson's ratio equals to 0.16 and  $\delta_{ij}$  is the Dirac delta function. In order to make the simulation simple and convenient,  $\lambda$  is set to be 0.5 in this letter. At 100 K,  $\Delta f(T) = 2.89 \times 10^7$  J/m<sup>3</sup>,  $A^* = 0.643 \ 2$ ,  $B^* = 2.840$ ,  $C^* = 1.330$ ,  $\varepsilon_0(T) = -0.011 \ 35$ ,  $L^* = 0.15$ <sup>[12]</sup>. We use the reduced time  $\Delta \tau = 0.02$  and  $N_0 = 64$  of computational cell with periodic boundary condition.

## 3 Results and discussions

Figure 1 shows that when the external compressive stress ( $\sigma$ ) is less than 12 GPa, the relative volume fractions  $\zeta$  ( $\zeta = (Vol - Vol_0) / Vol_0$ ,  $Vol$  is the volume fraction under stress and  $Vol_0$  is the volume fraction of initial state) of variant 2 ( $V_2$ ) and variant 3 ( $V_3$ ) increase with  $\sigma$ , while the relative volume fractions of variant 1 ( $V_1$ ) decrease with  $\sigma$ . This can be explained from the Bain strain matrix of three variants that each variant expands along its main axis and compresses along other two axis. If  $\sigma$  is applied along  $[100]$  direction,  $V_1$  will degenerate and transform into  $V_2$  and  $V_3$  through the interfacial migration (twin boundary), compared A (the initial state) and C (the metal-stable state under 6 GPa) in the

Figure 1. It is easy to find that the thin plate of  $V_2$  or  $V_3$  is apparently thickened when the morphology A evolves to C. Twin boundary will play an important role in realizing the re-orientation of different variants in this case. If  $\sigma > 10$  GPa,  $V_1$  vanishes while  $V_2$  and  $V_3$  will be left in the system. For example, the morphology of B in the Figure 1 includes only two variants if the compressive stress of 20 GPa is applied to the system. Compared B with A and C,  $V_2$  and  $V_3$  can be redistributed through altering the internal stress state of the system, which is helpful to get the good shape memory effect by using mechanical training.

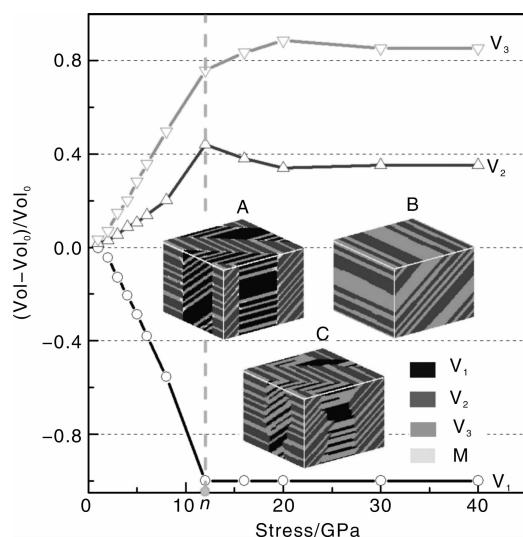


Figure 1 Volume fraction of three variants varying with the external compressive stress

Zhang *et al.*<sup>[1-2]</sup> found two-way SME in Mn-based alloys and there were good SME after 60 stress-cycles. The main mechanism is to get the reliable group of variants under the mechanical training, which is in accordance with other SMAs. Figure 2 gave the information about the micro-structural evolution during the 100 stress cycles. The detailed procedure is as follows, the external stress of 20 GPa was added in the initial state (A in Figure 1) and relaxed for about 6 000 steps to the metal-stable state under the stress, then the stress was moved and the system without loading was relaxing for another 6 000 and arrived at another free state. This was called one stress-cycle. One most important character in Figure 2 is that the vanished  $V_1$  appeared in the system after removing the loading, compared (b), (d), (f) and (h) with the corresponding (a), (c), (e) and (g). This kind of phenomenon has good memory effect during the 100 cycles, though their morphology and location have a little difference. The nucleation and growth of  $V_1$  in  $V_2$  and  $V_3$  may make a great contribution to this kind of difference. Comparing (a) in Figure 2 with B in Figure 1, we find  $V_3$  becomes thicker and some thicker plates of  $V_3$  disappears after 25 loading cycles. The external stress will lead to the reorientation and redistribution of the variants in the considered system.

At the first 5 cycles ( $n_0 = 5$ ), the volume fractions of three variants have a great change, shown in Figure 2i. Their morphology (in Figure 1A and Figure 2a) will also have a difference. When  $n_0 > 5$ , the volume fraction of each variant has a very small fluctuation without big change, which exhib-

its the memory effect of volume. The main goal of mechanical training is to obtain the single variant so as to enhance the SME. Based on the above analyses, the bigger external stress ( $> 10$  GPa) is applied along  $[100]$  direction and two variant will be obtained in the system under the stress state. But the state of only two variants can not be kept in the stress-free state, which may be different from the mechanism of training<sup>[13]</sup>. Here we want to propose a possible viewpoint to explain the mechanism of mechanical training that the cyclic stress reorients and redistributes the martensitic variants to make the phase transformation more regular and the volume fractions of variants have the memory effect so as to guarantee the good SME.

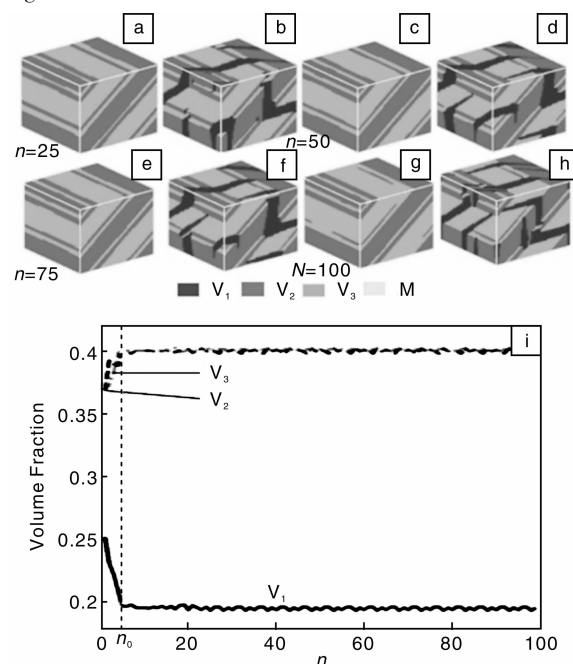


Figure 2 The micro-structural evolution under cyclic loading (a), (c), (e) and (g), and without loading (b), (d), (f) and (h). (i) Vol varying with  $n$  after removing the loading

The transformation mechanism of A→C may be different from that of A→B (shown in Figure 1). When the external stress is applied in the system,  $V_1$  will immediately transform into parent (shown in Figure 3a). In other words, the parent can nucleate at the twin boundary of two martensitic variants and grow quickly. Then the parent disappears step by step with the increasing the time under the stress, which depends on the motion of martensite/parent interface. This kind of interfacial migration is different from the above mechanism of twin-boundary motion (C shown in Figure 1), which may be due to the faster response of interface under bigger loading rather than the slower response of twin boundary under the smaller loading. It is interesting to find that the  $V_1$  can nucleate at the twin boundary of  $V_2$  and  $V_3$  and can grow and pass through the twin boundary, shown in Figure 3b. Because of the sites of martensitic nucleation at the twin boundary, the morphological of the system without loading exhibits a little difference in Figure 2a, d, f and h. Tanaka *et al.* observed the interfacial motion under stress<sup>[14]</sup> and Lai *et al.* observed the twin-boundary migration under the magnetic field<sup>[4]</sup>. But no experimental results gave the direct observation of the re-

orientation of martensitic variants. Our simulated microstructural evolution of martensitic variants will provide a good base consideration of mechanism of reorientation and redistribution of multi-variants.

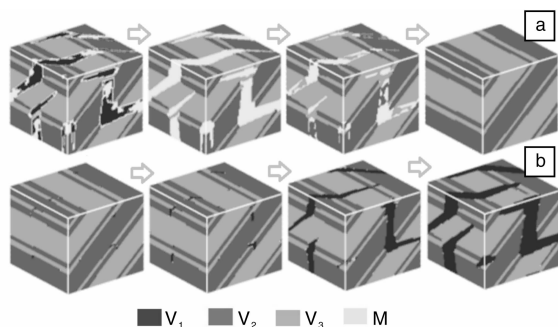


Figure 3 The micro-structural evolution of three variants under the 75<sup>th</sup> loading (a) and the nucleation and growth of variant 1 after removing the loading (b)

As for the interfacial nucleation of  $V_1$  shown in Figure 3b, the energy evolution of the system will help us understand the physical nature of phase transition (shown in Figure 4). This procedure can be divided into three zones:  $Z_1$ ,  $Z_2$  and  $Z_3$ , which corresponds to the incubation stage, nucleation stage and growth stage, respectively. At the first stage,  $F_{el}$  decreases with the time while the other energies have little variation, which releases the strain energy and decreases the stress concentration at the twin boundary. The nucleation of  $V_1$  mainly occurs at the second stage, because  $F_{el}$ ,  $F_{int}$ , and  $F_{ch}$  of system vary greatly. Compared with the length of the first stage, this procedure becomes faster. However, at the third stage, the variation of each energy slows down and the growth of  $V_1$  costs more time than the first two stages. In fact, the nucleation of martensite is rather quick than the growth so as not to capture this procedure easily in the experiments. In this paper, the twin-boundary nucleation mechanism was simulated successfully and needs more future experimental observation.

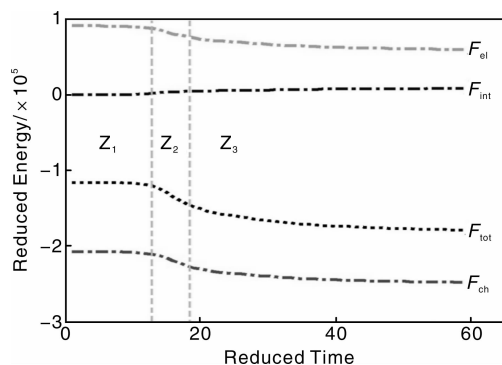


Figure 4 The reduced strain energy ( $F_{el}$ ), interfacial energy ( $F_{int}$ ), chemical energy ( $F_{ch}$ ) and total energy ( $F_{tot}$ ) varying with the reduced time

## 4 Conclusions

In conclusion, a twin boundary model was introduced into the phase-field method to investigate the mechanism of

reorientation and redistribution of martensitic variants under the external field. The results of simulation show that the twin boundary migration is the main mechanism to perform the altering of variants under the small loading. If the external stress exceeds one critical value, the parent phase with three variants will nucleate at the twin-boundary and grow quickly, then transform into two variants by means of the motion of martensite/parent interface. After removing loading, the vanished variant will nucleate and grow at the twin boundary to finish the redistribution of inner micro-structure. This kind of mechanism controls the shape memory effect of the Mn-Cu alloy during the cyclic loading.

## Acknowledgements

Thank Dr. Guo Zhengong for the useful discussion.

## References

- [1] Zhang J H, Peng W Y, Hsu T Y. The Magnetic Field Induced Strain without Prestress and with Stress in a Polycrystalline Mn-Fe-Cu Antiferromagnetic Alloy[J]. *Appl Phys Lett*, 2008, 93: 122 510 - 122 512.
- [2] Zhang J H, Rong Y H, Hsu T Y. The Coupling between First-Order Martensitic Transformation and Second-Order Antiferromagnetic Transition in Mn-Rich  $\gamma$ -MnFe Alloy[J]. *Phil Mag*, 2010, 90: 159 - 168.
- [3] Tian Q C, Yin F X, Takuya S, *et al.* Reverse Transformation Behavior of a Prestrained MnCu Alloy[J]. *Acta Mater*, 2006, 54: 1 805 - 1 813.
- [4] Lai Y W, Scheerbaum N, Hinz D, *et al.* Absence of Magnetic Domain Wall Motion During Magnetic Field Induced Twin Boundary Motion in Bulk Magnetic Shape Memory Alloys[J]. *Appl Phys Lett*, 2007, 90: 192 504 - 192 506.
- [5] Skumryev V, Laukhin V, Fina I, *et al.* Magnetization Reversal by Electric-Field Decoupling of Magnetic and Ferroelectric Domain Walls in Multiferroic-Based Heterostructures[J]. *Phys Rev Lett*, 2011, 106: 057 206.
- [6] Wang D, Wang Y, Zhang Z, *et al.* Modeling Abnormal Strain States in Ferroelastic Systems; the Role of Point Defects[J]. *Phys Rev Lett*, 2000, 105: 205 702.
- [7] Artemev A, Wang Y, Khachaturyan A G. Three-Dimensional Phase Field Model and Simulation of Martensitic Transformation in Multilayer Systems under Applied Stresses[J]. *Acta Mater*, 2000, 48: 2 503.
- [8] Levitas V I, Preston D L. Three-Dimensional Landau Theory for Multivariant Stress-Induced Martensitic Phase Transformations[J]. *Phys Rev B*, 2002, 66: 134 206 - 134 207.
- [9] Zhang W, Jin Y M, Khachaturyan A G. Phase Field Microelasticity Modeling of Heterogeneous Nucleation and Growth in Martensitic Alloys[J]. *Acta Mater*, 2007, 55: 565 - 574.
- [10] Chen L Q, Shen J. Applications of Semi-Implicit Fourier-Spectral Method to Phase Field Equations[J]. *Comp Phys Commu*, 1998, 108: 147 - 158.
- [11] Fukuhara M, Yin F X, Ohsawa Y, *et al.* High-Damping Properties of Mn-Cu Sintered Alloys[J]. *Mater Sci & Eng A*, 2006, 442: 439 - 443.
- [12] Man J, Zhang J H, Rong Y H. Microstructural Evolution of Mn-Rich Antiferromagnetic Mn-Cu Alloy under Temperature Field[J]. *Appl Phys Lett*, 2010, 96: 131 904 - 131 906.
- [13] Saburi T, Nenno S, Wayman C M. *Proceeding. ICOMAT-79* [C]. Cambridge MA: MIT, 1979: 619.
- [14] Tanaka Y, Himuro Y, Kainuma R, *et al.* Ferrous Polycrystalline Shape-Memory Alloy Showing Huge Superelasticity[J]. *Science*, 2010, 327(5 972)1 488 - 1 490.